Regular Article

PHYSICAL CHEMISTRY RESEARCH
Published by the
Iranian Chemical Society
www.physchemres.org
info@physchemres.org

***Phys. Chem. Res.**, Vol. 6, No. 4, 795-804, December 2018*
DOI: 10.22036/pcr.2018.132457.1488

Effects of Functionalization of Carbon Nanotubes on Activity and Selectivity of Co/CNT Catalysts in Fischer-Tropsch Synthesis

B. Hatami[a], A. Asghari[a,*], A. Tavasoli[b], Y. Zamani[c] and A. Zamaniyan[c]

[a]*Department of Chemistry, Semnan University, Semnan, Iran*
[b]*School of Chemistry, College of Science, University of Tehran, Tehran, Iran*
[c]*Gas Research Division, Research Institute of Petroleum Industry, Tehran, Iran*

(Received 30 April 2018, Accepted 19 September 2018)

The Fischer-Tropsch Synthesis (FTS) activities of cobalt-based catalysts supported on carbon nanotubes (CNTs) and functionalized carbon nanotubes (FCNTs) are investigated in this work. The cobalt-based catalysts are synthesized by the reverse micro-emulsion technique using a non-ionic surfactant, and characterized by the Brunauer-Emmett-Teller, X-ray diffraction, H_2 chemisorption, temperature program reduction, and transmission electron microscopy techniques. The activities of the synthesized catalysts are evaluated in terms of the FTS production rate (g produced hydrocarbons/g.cat./h) and selectivity (percentage of the CO converted to hydrocarbon products). According to the TEM results, the synthesized cobalt nanoparticles have a narrow size distribution and are mostly confined inside the functionalized CNTs (FCNTs). These nanoparticles are highly reducible as evidenced by the reduction peaks of the FCNT catalyst shifting to low temperatures. In comparison to non-functionalized CNT, FCNT increases the FTS rate and CH_4 selectivity, and decreases the C_5^+ selectivity as a catalytic support. In addition, the FCNT support preserves the high dispersion and reducibility of cobaltthat can be attributed to the hydrogen spill-over effect of the functional groups present on the CNT surface.

Keywords: Nanoparticle dispersion, Carbon nanotubes, Fischer-Tropsch synthesis, Functionalization

INTRODUCTION

In the recent years, the demand for fossil fuels has raised the focus on the Fischer-Tropsch synthesis (FTS) in both academia and industry [1-3]. In the FTS reaction, the syngas (a mixture of CO and H_2) is changed into liquid hydrocarbons *via* catalytic surface polymerization. Supported cobalt catalysts are famous in the FTS process due to their high activity and selectivity towards paraffinic hydrocarbons. High chain growth probability, low deactivation rate, and small water-gas shift activity are among the reasons for choosing the cobalt-based catalysts as the best options for converting the syngas into clean liquid fuels [4,5].

It is well-recognized that the size, dispersion, and reduction degree of the catalyst particles are important parameters for the CO hydrogenation mechanism [6]. These characteristics are influenced by the support selection in cobalt-based catalysts. Nowadays, the use of carbon supports, due to their suitable surface properties, is very much considered in the catalyst preparation. Nevertheless, these types of supports have small interactions with the cobalt active phase. In the carbon nanotube (CNT)-supported cobalt catalyst, the strong metal-support interactions are decreased to a large degree [7,8]. It is well-known that the synthesis of highly dispersed and stable cobalt catalysts requires strong interactions between the support and the cobalt active phase [9], making CNTs an unsuitable support in cobalt-based catalysts. Functionalization of CNTs as a support is a new technique for the catalyst preparation. This process allows the control of metal particle size with a narrow size distribution due to

*Corresponding author. E-mail: aasghari@semnan.ac.ir

the rise in the support interaction with the cobalt active phase [6].

Despite the fact that functionalization of the supports extremely influences the interaction between the cobalt particles and the CNT support, the functional groups formed on the surface of CNT support cause the sintering of cobalt particles [9]. Alternatively, the concentration, distribution and nature of the functional groups present on the surface of CNTs play an important role in the dispersion of the metal particles on the CNT support [9]. Chen et al. have reported that the confinement of the iron particles inside CNTs leads to a high reducibility and a superior CO dissociative adsorption on the metal surface [10]. For the CNT support with open cap, capillary force leads to the confinement of cobalt particles inside the CNT pores [7,11]. Thus, a cobalt active site located inside the tubes must be more active than the one located on the external surface of the CNT support [12].

The aim of this work is to evaluate the effect of functionalization of the CNT support on the activity and selectivity of the cobalt-based catalyst in the FTS reaction. The results obtained are compared with those of common CNTs used as the catalytic support. A detailed discussion is provided to draw useful scientific and technical conclusions.

EXPERIMENTAL

Catalyst Preparation

Purified multi-walled CNTs were synthesized based on a method described in detail in Ref. [12]. The purity of the prepared CNTs was about 95%, and their diameters and lengths were in the ranges of 10-20 nm and 5-15 μm, respectively [13]. For the chemical functionalization procedure of CNTs, about 1 g of the purified CNTs was added to 150 ml H_2O_2 (30%) and sonicated for 15 min [6]. Then, a stream of the ozone gas was continuously passed through the mixture at a rate of 300 ml min^{-1} for 4 h. The prepared support precursor was filtered and washed with methanol to eliminate the residual H_2O_2, and then dried at 120 °C for 5 h.

The pure and functionalized CNTs were used as the supports for the preparation of the cobalt-based catalysts. These catalysts (15 wt% cobalt loaded) were prepared by the reverse micro-emulsion method using a solution of cobalt nitrate ($CO(NO_3)_2.6H_2O$, 99%, Merck), the non-ionic surfactant Triton X-100 (Chem-Lab), n-hexane (C_6H_{14}, Chem-Lab) as the oil phase, and 1-butanol (C_4H_9OH, Merck) as the co-surfactant [4]. The water-to-surfactant molar ratio (W/S) was set at 0.5. The catalyst precursors were filtered and washed with distilled water and ethanol. Then, the catalysts dried at 120 °C for 2 h, and calcined under an argon atmosphere at 450 °C for 3 h.

Catalyst Characterization

FT-IR spectra were obtained by a Bruker ISS-88. A smooth transparent pellet of 2.5% of CNTs mixed with 97.5% KBr was made, and the IR beam was passed through this pellet. The surface area, pore volume, and pore average diameter of the calcined catalyst were measured using an ASAP-2010 Micrometrics system [14]. The morphologies of the calcined catalysts were considered by transmission electron microscopy (TEM) using a Philips CM20 (100 kV) equipped with a NARON energy-dispersive spectrometer and a germanium detector.

The prepared cobalt oxide phases and the cobalt crystallite size in the catalyst were analyzed by XRD using a Philips Analytical X-ray diffractometer (XPert MPD) with monochromatized Cu/Kα radiation between 2θ angles from 20° to 80°. The Debye-Scherer formula was used for the Co_3O_4 peak at 2θ = 36.8° in order to calculate the average cobalt crystallite size.

The H_2-TPR technique was performed in order to study the reducibility of the catalysts [5]. 0.05 g of the calcined catalyst sample was purged under a helium flow at 140 °C. Then, TPR of the sample was performed using 5% H_2 in an argon stream at a flow rate of 40 ml min^{-1} at atmospheric pressure using a Micrometrics TPD-TPR 2900 analyzer equipped with a thermal conductivity detector (TCD), heating at a linearly programmed rate of 10 °C min^{-1} up to 850 °C.

The hydrogen chemisorption of the fresh and used catalysts was conducted using the Micromeritics TPD-TPR 290 system. About 0.25 g of the sample was reduced under a hydrogen flow at 400 °C for 12 h. Then, the sample was purged by argon in order to remove the weakly adsorbed hydrogen. Finally, the temperature programmed desorption (TPD) of the sample was obtained with a heating ramp of 10 °C min^{-1} to 400 °C under an argon flow.

Catalyst Activity Test

The FTS activity (g HC produced/g cat./h) and product selectivity were evaluated using a fixed bed tubular stainless steel micro-reactor of 20 mm internal diameter. Three mass flow controllers (Brooks, Model 5850E) were used to control the flow rate of the inlet gases (CO, H_2 and N_2 with a purity of 99.999%), and a mechanical back-pressure regulator was used to control the pressure of the system. Three thermocouples were located in the catalyst bed for monitoring the inlet, outlet, and bed temperatures. The meshed catalyst (1.0 g) was held in the center of the reactor and diluted using quartz wool. The catalysts were reduced in hydrogen at 400 °C and atmospheric pressure for 16 h before the FTS reaction. The FTS reaction was carried out in T = 220 °C, H_2/CO = 2, P = 2.5 MPa and GHSV = 6000 h^{-1}. The reactants and products were analyzed using two chromatography devices equipped with a sample loop, a thermal conductivity detector (TCD), and a flame ionization detector (FID). Total mass balances were accepted if the carbon balance is closed between 98% and 102%. This criterion adopted since compounds containing carbon and hydrogen may accumulate in the reactor, in the form of high molecular weight hydrocarbons.

The CO conversion, FTS rate (g HC/g cat./h), and selectivity of the products were defined using the formula presented in our previous work [15]. The conversion of carbon monoxide was calculated as follows:

$$\%CO = \frac{CO_{in} - CO_{out}}{CO_{in}} \quad (1)$$

where CO_{in} is the amount of CO in reactor entrance and CO_{out} is the amount of CO in reactor output.

RESULTS AND DISCUSSION

CNT Characterization

Figure 1 shows the FT-IR spectra for the purified and functionalized CNTs, and their analysis results are shown in Table 1. According to Fig. 1 and Table 1, the purified and functionalized CNTs show the same absorption band around 1580 cm^{-1}, which can be attributed to the C=C stretching [6]. The coupling of functional groups to CNTs can be established by the existence of a series of new vibration bands at 3300-3600 cm^{-1} (OH) in the functionalized CNT spectrum. There is a peak around 1200 cm^{-1} for functionalized CNTs, which may be related to the C-O stretching of -COOH group. The broad peak at 1725 cm^{-1} may be attributed to the C=O group. In addition, the two peaks around 1400 and 3215 cm^{-1} may be related to the bending and stretching vibrations of the O-H group, respectively. The presence of these peaks may be corroborated by the fact that the carboxylic groups have been effectively prepared on the surface of functionalized CNTs during the acid treatment. The peaks at 2850-2950 cm^{-1} (both C-H anti-symmetric and symmetric stretches for CH_3 and CH_2) and 597 cm^{-1} (C-H) are shown in Fig. 1 [16]. There is a peak at 597 cm^{-1} that is related to the C-H bending mode, and represents the formation of defects in the process of functionalization of the CNT support.

Catalyst Characterization

The BET surface area and the average pore size for the fresh calcined catalysts and purified CNT support are shown in Table 1. As shown in this table, the BET surface area of the freshly prepared cobalt catalysts are lower than that of the CNT support, demonstrating some pore obstacles by cobalt oxide particles in the CNT pores.

The XRD patterns for the calcined catalysts are shown in Fig. 2. In the XRD patterns for both catalysts, the peaks located at 2θ = 25° and 43° correspond to the CNT support, whereas the other peaks are associated to the different crystal planes of Co_3O_4 [17]. As shown in Fig. 2, the peak at 2θ = 36.8° is the most strong one for the Co_3O_4 crystal in the XRD patterns for the catalysts. Minor peaks at 44° and 52° are correlated with a cubic cobalt structure [18]. Table 1 also reveals the average Co_3O_4 crystallite size of the catalysts, calculated using the Scherer formula (for the peak located on 2θ = 36.8°) [17]. As shown in Table 1, the average Co_3O_4 crystallite size is equal to 14.7 nm and 13.1 nm for Co-CNTs and Co-FCNTs, respectively. The metallic cobalt crystallite size was calculated to be about 11.0 nm and 9.8 nm, when Co_3O_4 is reduced to Co, respectively.

The TEM image for the catalysts is shown in Fig. 3. This image demonstrates the presence of cobalt nanoparticles inside and outside of the CNT channels. The cobalt nanoparticles inside the CNT channels were papered due to diffusion of solvent into the channels, and capillary

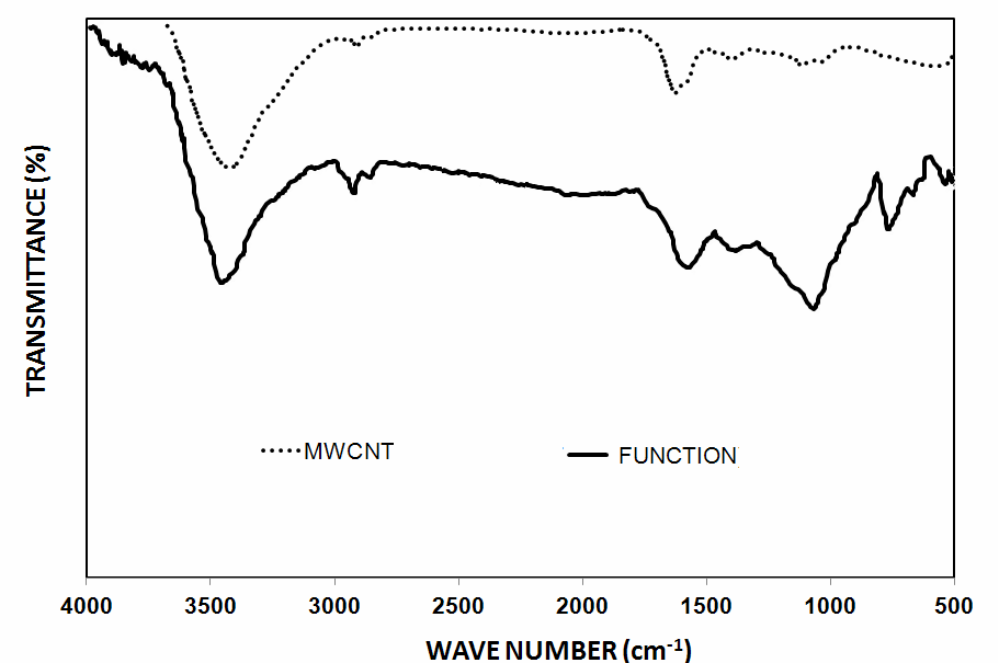

Fig. 1. FT-IR spectra for multi-walled CNTs and functionalized multi-walled CNTs.

Table 1. Spectral Analysis of FT-IR Peaks

Functional group	Type of vibration	Characteristic absorption range (cm^{-1})
C=C	Stretching	1580
C=O	Stretching	1725
C-O	Stretching	1200
O-H	Stretching	3215
O-H	Bending	1400

forces led to the confinement of cobalt particles inside the CNT channels [7]. As shown in Fig. 3, the cobalt content inside FCNTs is higher than that in the CNT support. The inner diameter of CNTs (10 nm) controlled the insertion of larger cobalt particles into the channel diameter. Thus, all particles with dimensions larger than 10 nm lie on the outer surface of the CNT walls. The size distribution of the cobalt particles was determined based on the data taken from different TEM images (Fig. 3). As shown in this figure, the functionalized CNT support enables us to control a narrow cobalt nanoparticle size distribution [6].

The reducibility of the prepared catalysts was determined by the TPR experiments (Fig. 4). In this figure, the low temperature peak is normally assigned to the reduction of Co_3O_4 to CoO [19]. The second wide reduction peak is related to the reduction of CoO to Co. The cobalt

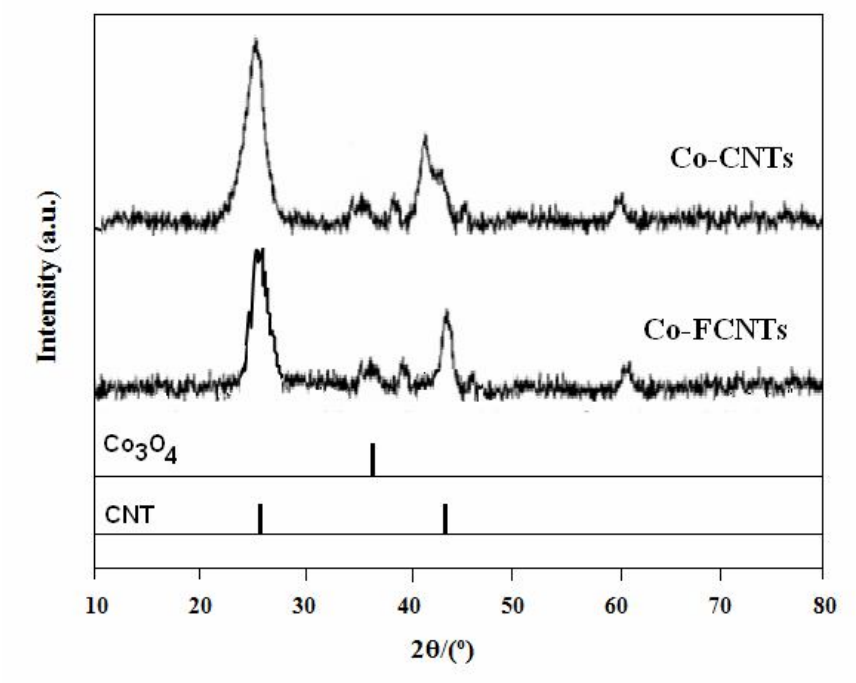

Fig. 2. XRD patterns for calcined catalysts.

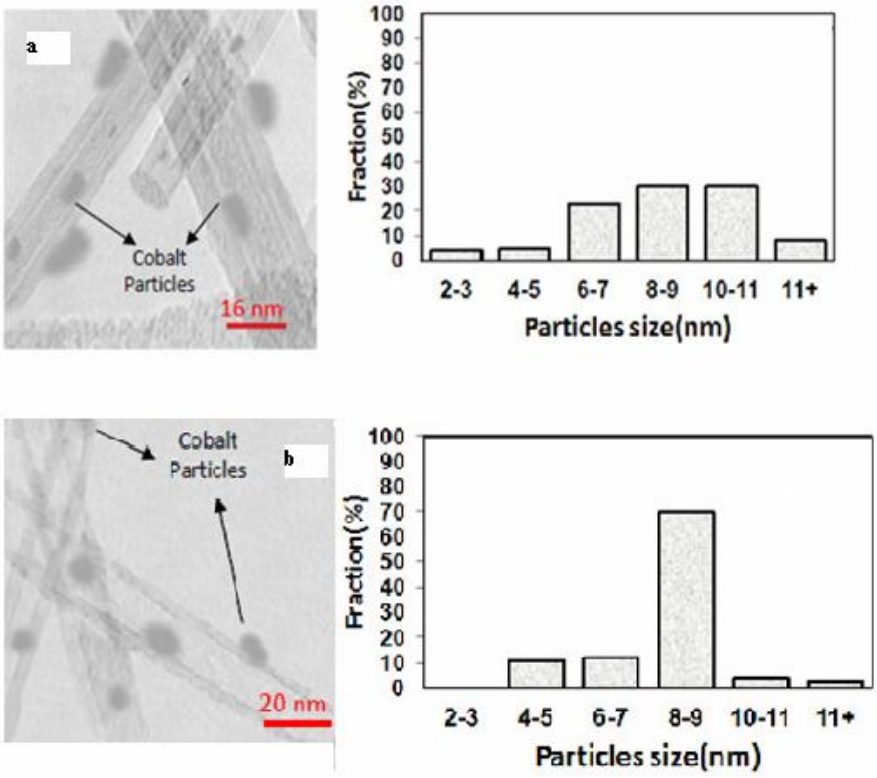

Fig. 3. TEM images and particles size distributions for calcined catalysts. a) Co-CNT; b) Co-FCNT.

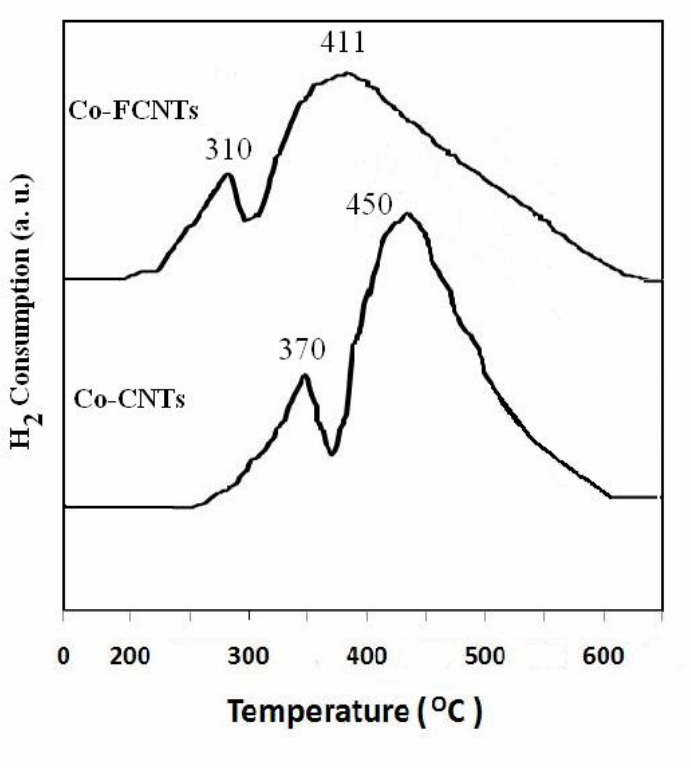

Fig. 4. TPR patterns for calcined catalysts.

Table 2. Chemical Composition and Textural Properties of Calcined Catalysts

Catalyst	Support	BET surface area ($m^2 g^{-1}$)	Total pore volume ($ml g^{-1}$)	Average pore diameter (Á)	Degree of reduction (%)
CNTs	-	216	0.56	112	-
Co-CNTs	CNTs	98	0.33	137	63
Co-FCNTs	Functional CNTs	135	0.41	116	71

particles located on the surface of functionalized CNTs will be easily reduced due to the confinement phenomenon and hydrogen spill-over of the functional groups. In addition, it can be recognized that the external surfaces of CNTs are electron-rich, while the inner ones are electron-poor [20]. Confinement of the cobalt nanoparticles (as shown in Fig. 3) inside CNTs will lead to a particular interaction between the inner nanotube surfaces and the metal particles. The degree of reduction of the cobalt oxides is the ratio of hydrogen consumed during reduction to the theoretical amount of hydrogen for the complete reduction of cobalt oxides. The degree of reduction of the cobalt catalysts are reported in Table 2. As shown in this table, the degree of reduction for Co-FCNTs catalyst is higher than that for Co-CNTs catalyst.

According to Fig. 3, the reduction peaks for cobalt nanoparticles located on the functionalized CNTs support shift to a lower temperature compared to the catalyst

Table 3. H_2 Uptake, Dispersion (%), and Average Co Particle Size of Catalysts

Catalyst	H_2 uptake[a]	Dispersion (%)		dp Co (nm)			
		XRD results	H_2 TPD	XRD results	TEM average	H_2 TPD	
						Fresh catalyst	Used catalyst
Co-CNTs	114	8.7	8.6	11.0	10.9	11.2	14.1
Co-FCNTs	146	9.8	9.9	9.8	9.6	9.7	12.9

[a](μmole H_2 desorbed/g_{cat}).

Table 4. CO Conversion, Chain Growth Probability, and Hydrocarbon Selectivities Calculated after 25-30 h on Stream (T = 220 °C, P = 25 bar, H_2/CO = 2.0 and GHSV = 6000 h^{-1})

Catalyst	CO Conversion (%)	α	FTS rate (g_{HC}/g_{cat}/h)	Selectivity (%)				
				CH_4	C_2-C_4	C_5-C_{12}	C_{13}-C_{19}	C_{20+}
Co/CNTs	45	0.87	0.81	11.2	26.6	38.6	14.5	9.1
Co/FCNTs	57	0.82	0.87	14.4	30.9	36.5	11.3	7.0

prepared on a common CNT. This event may be related to the higher reducibility of uniform cobalt particles produced on the functionalized CNTs support. The prepared functional groups on the CNT support have obstructed the sintering of cobalt and accelerated the hydrogen spill-over effect in the reduction process.

The results of the hydrogen chemisorption of the fresh and used catalysts using temperature programmed desorption (TPD) technique are reported in Table 3. As shown in Table 3, H_2 desorptions are 114 to 146 μmole H_2 desorbed/g_{cat} for Co-CNTs and Co-FCNTs fresh catalysts, respectively. Hydrogen chemisorption data were employed to determine cobalt dispersion and anticipate metal particle size. As shown in Table 3, the cobalt particle size are increased from 9.7 to 11.2 nm for Co-FCNTs and Co-CNTs fresh catalysts, respectively. These results show that the hydrogen uptake of the Co-FCNT catalyst is higher than that of the Co-CNT catalyst due to the narrow particle size distributions in the Co-FCNT catalyst [21]. Bezemer *et al.* have reported that the hydrogen uptake is directly associated to the cobalt particle size for particles less than 10 nm, a trend that levels off for bigger particles [1]. Table 3 also shows that the cobalt particle size is increased after reaction due to cobalt sintering. The cobalt particle size increased from 9.7 to 12.9 nm for Co-FCNTs and 11.2 to 14.1 nm for Co-CNTs catalyst.

FTS Activity

The relative results of carbon monoxide conversion, product selectivity, and FTS rate (g HC produced/g cat./h)

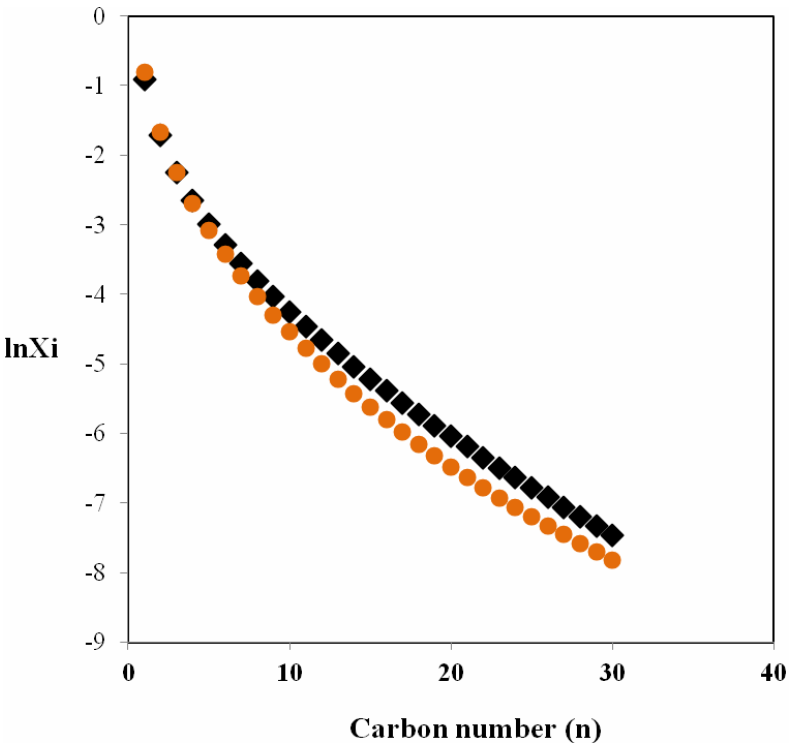

Fig. 5. Chain length distribution over calcined catalysts; T = 220 °C, H_2 /CO = 2, P = 2.5 MPa, Xi mole fraction of component i. ●: Co-FCNT; ■: Co-CNTs.

for the Co-CNT and Co-FCNT catalysts are presented in Table 4. As shown in this table, the Co-FCNT catalyst show higher FTS rate, CO conversion and higher selectivity to light hydrocarbons such as methane and C_2-C_4 hydrocarbons. However, the Co-CNT catalyst shows higher C_5^+ selectivity. The selectivity to light hydrocarbons is related to the concentration of monomers that exhibited higher degree of hydrogenation (like CH_2 species) on the surface of catalyst [22]. Although, the selectivity to heavy hydrocarbons is related to the concentration of monomers that exhibited lower degree of hydrogenation (like HCO, HCOH species) on the surface of catalyst [22]. The concentration of monomers that with higher degree of hydrogenation is increased with decreasing the catalyst particle size [22]. As reported in the previous section, the Co-FCNT catalyst has a narrow and uniform particle size distribution. In addition, the cobalt nanoparticles are mostly inside CNTs. The cobalt sites produced inside the functionalized CNTs are more stable and more catalytically active than the ones produced on common CNTs [4,8,9,11]. These functional groups are considered as the anchoring sites for metal particles on the inner and outer graphite layers of CNTs, affecting the metal dispersion and stability of active metallic sites [10]. As shown in Table 4, improvement in the uniformity of the cobalt particles supported on functionalized CNTs leads to an increase in the FTS activity and stability of the catalyst. These results reveal that the FTS activity of the catalysts is strongly dependent on the size distribution of the cobalt particles, and the effect of cobalt particle confinement within the functionalized CNTs on the FTS activity may be more important than that of the particle size [9,11].

The chain length distribution of the FTS products for cobalt-based catalysts can be well-characterized by the two ASF distributions in Fig. 5 [22]. As shown in Table 4, the chain growth probability was 0.82 and 0.87 for the Co-FCNT and Co-CNT catalysts, respectively. These results show that the Co-CNT catalyst with a larger cobalt particle

size produces heavier hydrocarbons due to the steric hindrance. Large particles (+10 nm) have a high potential of re-adsorption and polymer chain initiation on the catalyst surface [2,4].

CONCLUSIONS

In this work, we compared the effects of CNT functionalization on the cobalt catalyst preparation and FTS reaction for catalysts with 15 wt% cobalt loadings. According to the TEM results, the cobalt nanoparticles produced on the functionalized CNTs showed a narrow particle size distribution. According to the TPR results of the functionalized CNTs, the reduction steps shifted to a lower temperature compared to non-functionalized CNTs, likely due to the hydrogen spill-over effect of the functional groups on the CNT surface. The catalytic results showed that the FTS activity and product selectivity were strongly dependent on the cobalt particle size distribution. However, the effect of cobalt particle confinement within the functionalized CNTs on the FTS activity may be more important than that of the particle size. As a result, using the catalyst particles supported on functionalized CNTs led to a higher CO conversion and FTS activity compared to those prepared on common CNTs.

REFERENCES

[1] Bezemer, G. L.; Bitter, J. H.; Kuipers, H. P. C. E.; Oosterbeek, H.; Holewijn, J. E.; Xu, X.; Kapteijn, F.; Jose van Dillen, A.; De Jong, K. P.; Cobalt particle size effects in the Fischer-Tropsch reaction studied with carbon nanofiber supported catalysts. *J. Am. Chem. Soc.* **2006**, *128*, 3956-64, DOI: 10.1021/ja058282w.

[2] Nakhaei Pour, A.; Dolati, F., Activation energies for chain growth propagation and termination in Fischer-Tropsch synthesis on iron catalyst as a function of catalyst particle size. *Prog. React. Kinet. Mech.* **2016**, *41*, 371-384, DOI: 10.3184/174751916X14701459562861.

[3] Nakhaei Pour, A.; Housaindokht, M. R.; Monhemi, H., A new LHHW kinetic model for CO_2 hydrogenation over an iron Catalyst. *Prog. React. Kinet. Mech.* **2016**, *41*, 159-169. DOI: 10.3184/146867816X14628763021337.

[4] Trépanier, M.; Tavasoli, A.; Dalai, A. K.; Abatzoglou, N., Fischer-Tropsch synthesis over carbon nanotubes supported cobalt catalysts in a fixed bed reactor: Influence of acid treatment. *Fuel Processing Technol.* **2009**, *90*, 367-374, DOI: 0.1016/j.fuproc.2008.10.012.

[5] Tavasoli, A.; Nakhaei Pour, A.; Ghalbi Ahangari, M., Kinetics and product distribution studies on ruthenium-promoted cobalt/alumina Fischer-Tropsch synthesis catalyst. *J. Nat. Gas Chem.* **2010**, *19*, 653-9, DOI: 10.1016/S1003-9953(09)60133-X.

[6] Davari, M.; Karimi, S.; Tavasoli, A.; Karimi, A., Enhancement of activity, selectivity and stability of CNTs-supported cobalt catalyst in Fischer-Tropsch *via* CNTs functionalization. *Appl. Catal. A. Gen.* **2014**, *485*, 133-142, DOI: 10.1016/j.apcata.2014.07.023.

[7] Nakhaei Pour, A.; Karimi, J.; Taghipoor, S.; Gholizadeh, M.; Hashemian, M., Fischer-Tropsch synthesis over CNT-supported cobalt catalyst: Effect of magnetic field. *J. Iran. Chem. Soc.* **2017**, *14*, 1477-1488, DOI:

[8] Nakhaei Pour, A.; Karimi, J.; Torshizi, O.H., Hashemeian, M.; Kinetic study of Fischer-Tropsch synthesis using a Co/CNTs catalyst. *Prog. Reac. Kinet. Mech.* **2017**, *42*, 80-88, DOI: 10.3184/146867816X14799161258433.

[9] Zhang, Y.; Liu, Y.; Yang, G.; Endo, Y.; Tsubaki, N., The solvent effects during preparation of Fischer-Tropsch synthesis catalysts: Improvement of reducibility, dispersion of supported cobalt and stability of catalyst. *Catal. Today.* **2009**, *142*, 85-89, DOI: 10.1016/j.cattod.2009.01.014.

[10] Chen, W.; Fan, Z.; Pan, X.; Bao, X., Effect of confinement in carbon nanotubes on the activity of Fischer-Tropsch iron catalyst. *J. Am. Chem. Soc.* **2008**, *130*, 9414-9419, DOI: 10.1021/ja8008192.

[11] Abbaslou, R. M. M.; Tavasoli, A.; Dalai, A. K., Effect of pre-treatment on physico-chemical properties and stability of carbon nanotubes supported iron Fischer-Tropsch catalysts. *Appl. Catal. A. Gen.* **2009**, *355*, 33-41, DOI: doi.org/10.1016/j.apcata.2008.11.023.

[12] Pan, X.; Fan, Z.; Chen, W.; Ding, Y.; Luo, H.; Bao,

X., Enhanced ethanol production inside carbon-nanotube reactors containing catalytic particles. *Nat. Mater.* **2007**, *6*, 507-511, DOI: 10.1038/nmat1916.

[13] Karimi, A.; Nasernejad, B.; Rashidi, A. M.; Tavasoli, A.; Pourkhalil, M., Functional group effect on carbon nanotube (CNT)-supported cobalt catalysts in Fischer-Tropsch synthesis activity, selectivity and stability. *Fuel* **2014**, *117*, 1045-1051, DOI: 10.1016/j.fuel.2013.10.014.

[14] Tavasoli, A.; Trépanier, M.; Dalai, A. K.; Abatzoglou, N., Effects of confinement in carbon nanotubes on the activity, selectivity, and lifetime of Fischer-Tropsch Co/carbon nanotube catalysts. *J. Chem. Engin. Data* **2010**, 55, 2757-2763, DOI: 10.1021/je900984c.

[15] Karimi, A.; Nakhaei Pour, A.; Torabi, F.; Hatami, B.; Tavasoli, A.; Alaei, M. R.; Irani, M.; Fischer-Tropsch synthesis over ruthenium-promoted Co/Al_2O_3 catalyst with different reduction procedures. *J. Nat. Gas Chem.* **2010**, *19*, 503-508, DOI: 10.1016/S1003-9953(09)60111-0.

[16] Bezemer, G. L.; Radstake, P.; Koot, V.; Van Dillen, A.; Geus, J.; De Jong, K., Preparation of Fischer-Tropsch cobalt catalysts supported on carbon nanofibers and silica using homogeneous deposition-precipitation. *J. Catal.* **2006**, *237*, 291-302, DOI: 10.1016/j.jcat.2005.11.015.

[17] Nakhaei Pour, A.; Housaindokht, M. R., Fischer-Tropsch synthesis over CNT supported cobalt catalysts: Role of metal nanoparticle size on catalyst activity and products selectivity. *Catal. Lett.* **2013**, *143*, 1328-1338, DOI: 10.1007/s10562-013-1070-y.

[18] Chu, W.; Chernavskii, P. A.; Gengembre, L.; Pankina, G. A.; Fongarland, P.; Khodakov, A. Y., Cobalt species in promoted cobalt alumina-supported Fischer-Tropsch catalysts. *J. Catal.* **2007**, *252*, 215-230, DOI: 10.1016/j.jcat.2007.09.018.

[19] Das, T. K.; Conner, W. A.; Li, J.; Jacobs, G.; Dry, M. E., Davis, B. H., Fischer-Tropsch synthesis: Kinetics and effect of water for a Co/SiO_2 catalyst. *Energy & Fuels*. **2005**, *19*, 1430-1439, DOI: 10.1021/ef049869j.

[20] Nakhaei Pour, A.; Taheri, S. A.; Anahid, S.; Hatami, B.; Tavasoli, A., Deactivation studies of Co/CNTs catalyst in Fischer-Tropsch synthesis. *J. Nat. Gas Sci. Engin.* **2014**, *18*, 104-111, DOI: 10.1016/j.jngse.2014.01.019.

[21] Khodakov, A. Y.; Chu, W.; Fongarland, P., Advances in the development of novel cobalt Fischer-Tropsch catalysts for synthesis of long-chain hydrocarbons and clean fuels. *Chem. Rev.* **2007**, *107*, 1692-1744, DOI: 10.1021/cr050972v.

[22] Nakhaei Pour, A.; Housaindokht, M. R., Studies on product distribution of nanostructured iron catalyst in Fischer-Tropsch synthesis: Effect of catalyst particle size. *J. Indust. Engin. Chem.* **2014**, *20*, 591-6, DOI: 10.1016/j.jiec.2013.05.019.